PHYSICAL REVIEW D **93,** 035024 (2016)

Dark matter annihilation decay at the LHC

Yuhsin Tsai,[1] Lian-Tao Wang,[2,3] and Yue Zhao[4]

[1]*Maryland Center for Fundamental Physics, Department of Physics, University of Maryland, College Park, Maryland 20742, USA*

[2]*Department of Physics, The University of Chicago, Chicago, Illinois 60637, USA*

[3]*Enrico Fermi Institute and Kavli Institute for Cosmological Physics, The University of Chicago, Chicago, Illinois 60637, USA*

[4]*Michigan Center for Theoretical Physics, University of Michigan, Ann Arbor, Michigan 48109, USA*

(Received 7 January 2016; published 24 February 2016)

Collider experiments provide an opportunity to shed light on dark matter (DM) self-interactions. In this work, we study the possibility of generating DM bound states—the Darkonium—at the LHC and discuss how the annihilation decay of the Darkonium produces force carriers. We focus on two popular scenarios that contain large DM self-couplings: the Higgsinos in the λ-SUSY model and the self-interacting DM (SIDM) framework. After forming bound states, the DM particles annihilate into force mediators, which decay into the standard model particles either through a prompt or displaced process. This generates interesting signals for the heavy resonance search. We calculate the production rate of bound states and study the projected future constraints from the existing heavy resonance searches.

DOI: 10.1103/PhysRevD.93.035024

I. INTRODUCTION

The existence of dark matter (DM) has been proven by many astrophysical observations. However, all the supportive evidence so far comes from gravitational interactions between DM and standard model (SM) particles, and there is no direct and unambiguous evidence of other types of DM interactions yet. Many efforts, such as the direct and indirect detection experiments, have been devoted to search for the nongravitational DM-SM couplings. With no clear discoveries so far, it is important to look for other types of experiments that can provide a complimentary search.

Collider experiments serve this purpose well. Among the many advantages of looking for DM particles at colliders [1–4], one unique feature of these high energy experiments is that they provide a chance to study the mediators of DM interactions. Many papers have discussed looking for the mediator particles between the dark and SM sectors (see [5–7], for example). In this work, we instead study how the production of DM bound states at the Large Hadron Collider (LHC) can help to shed light on the DM self-interaction, which is mediated by a force carrier that couples strongly to the DM particle but weakly to the SM sector.

In this paper, we focus on two well-motivated scenarios that may naturally have strong DM self-interactions: the self-interacting dark matter models (SIDM) and λ-SUSY. DM self-interaction can impact the structures of DM halos [8]. Several astrophysical observations show potential deviations from theoretical predictions if only gravitational interaction of DM particles are included [9–12]. Moreover, detailed simulations show that some anomalies can be resolved by having self-interacting DM (SIDM) with a scattering cross section $\sigma/m_\chi \sim 0.1$–$10\ \mathrm{cm}^2/\mathrm{g}$ between DM particles [13–15]. Such a large cross section implies a strong DM self-interaction, which can come from the mediation of a light force carrier [16]. If the self-interaction is strong enough, DM bound states can be formed at colliders from the pair production of DM particles.

Likewise, the Higgs boson has been discovered at the LHC with a mass around 125 GeV [17,18]. The mass of the Higgs boson is too heavy to be naturally explained in the minimal supersymmetric SM (MSSM). With a variation to the superpotential, the λ-SUSY scenario introduces a large F term to the Higgs potential which helps to raise the Higgs mass [19,20]. The large value of λ implies a sizable attractive Yukawa coupling among Higgsinos and Singlino, mediated by the singlet scalar and Higgs boson. If the lightest neutralino, which serves as a good candidate for DM, is dominantly Higgsino and Singlino, the light force scalar mediator can also help to form a bound state when neutralinos or charged Higgsinos are pair produced.

A high energy collider provides special access to DM self-interactions. Once DM particles are produced near the threshold, there is a chance for them to form a bound state, the Darkonium, due to a strong self-interaction [21]. The particle and antiparticle in the bound state can easily find each other and annihilate into light mediators or SM particles. The collider signatures of forming a dark matter bound state is very different from the traditional DM search at colliders [28–33]. Instead of looking for missing energy and its recoiled objects, one can look for the resonance of the bound state. This greatly reduces the SM background and helps to extract information about the dark sector, such as reconstructing the mass of DM particles. Furthermore, the self-interaction force mediators can have a small coupling to the SM sector and negligible direct production

rates at colliders. The bound state production, however, can generate the force mediators from the bound state annihilation decay, which provides a plausible way to study the mediators [34].

Here we note that the collider production of DM bound state by the weakly interacted massive particles (WIMP) has been discussed in [37]. Different from their approach, we also study the possible bound state production in λ-SUSY, which is a well-motivated scenario. Further, we study the SIDM scenario with the input of preferred values of DM self-interaction strength, based on simulations. In Sec. II, we review the basics on calculations of the bound state production rate at a hadron collider. In Sec. III, we focus on the λ-SUSY scenario. Bound states are formed by neutralino/chargino. The neutralino/chargino production is through W/Z bosons and the singlet/Higgs bosons behave as the force mediators to form bound states. The annihilation decay products can be the mediator or W/Z bosons. We perform a simple PDF rescaling on existing similar searches at the LHC in order to get a rough estimation on the reach limit at higher energy and larger luminosity. In Sec. IV, we study the bound state from the SIDM model. The production of DM particles is calculated using effective operators, similar to the assumption in missing transverse energy (MET) searches. However, we emphasize that the constraints on the mediation scale of effective operator in MET searches can sometimes be much lower than the typical energy scale of the collision. Thus, there are concerns of self-consistency using the language of low energy effective theory. This problem is relieved in our scenario because the energy scale of our process is fixed to be the bound state mass. Finally, we summarize in Sec. V.

II. BOUND STATE PRODUCTION

We follow the technique in [38–40] to calculate the bound state production at the LHC. When the DM particles in a bound state are produced near the threshold, we can write the binding energy and wave function in terms of the DM mass m and self-coupling α_λ. For the s-wave bound state, we have

$$E_b = \frac{\alpha_\lambda^2 m}{4}, \qquad a_0^{-1} = \frac{1}{2}\alpha_\lambda m,$$
$$|\psi(0)|^2 = \frac{1}{\pi a_0^3} = \frac{\alpha_\lambda^3 m^3}{8\pi}, \qquad \mathcal{M}_b = \sqrt{\frac{1}{m}}\psi(0)\mathcal{M}_0, \tag{1}$$

where E_b is the binding energy, $\psi(0)$ is the wave function of DM particles at zero separation, $\mathcal{M}_0$ is the amplitude of producing two free DM particles, and $\mathcal{M}_b$ is the matrix element for generating a bound state. The self-coupling α_λ is obtained at the energy scale of the inverse Bohr radius a_0^{-1}. In the λ-SUSY discussion, we define λ to be the Higgsino-singlet Yukawa coupling at the Higgsino mass. Since there is no running of this particular Yukawa coupling below the mass scale, it is the α_λ to use for the bound state calculation. Similarly, we define the size of the SIDM coupling at the mediator mass, and there is no sizable running of the DM-mediator coupling down to the binding energy. We then do not include the running of the self-couplings in this work.

Equation (1) gives a nonrelativistic approximation of the DM particles in the bound state. The expression is valid when the constituent particles in the bound state have speed $v \sim \alpha_\lambda < 1$. Further, we need the light mediator wavelength to be longer than the Bohr radius, which requires $m_{\rm med} < \alpha_\lambda m/2$. The p wave has $\psi(0) = 0$, and the amplitude $\mathcal{M}_b$ depends on the derivative of $\psi(x)$ with respect to the radial coordinate. This gives a relative suppression $|\psi'(0)|^2/|\psi(0)|^2 \sim \alpha_\lambda^2$ for the bound state production and decay compared to the s-wave state. We then do not discuss the p wave or higher angular-excited states in this work.

To obtain the bound state production rate, we first calculate the amplitude of having free partons χ scattering into the SM quarks $\chi\bar{\chi} \to q\bar{q}$. According to the total angular momentum of the bound state, we use the corresponding wave function of each χ in spinor space in the nonrelativistic limit while keeping the quark wave function in the relativistic form. Summing the nonvanishing combinations of the spin polarization, the decay rate, $\Gamma_{\mathbf{B}\to q\bar{q}}$, can be calculated through $\mathcal{M}_b$. Averaging over the bound state polarization, one obtains the bound state production cross section as [39]

$$\sigma(q\bar{q} \to \mathbf{B}) = \zeta(3)\frac{4\pi^2(2J+1)}{9M^3}\mathcal{L}_{q\bar{q}}(M^2)\Gamma_{\mathbf{B}\to q\bar{q}}, \tag{2}$$

where $M \simeq 2m$ is the mass of the DM bound state. Here, $\zeta(3)$ comes from summing the modes of radial excitations. In principle, the sum should stop once the Bohr radius of radial excitation states is longer than the Compton wavelength of the mediator. But it only causes a difference of $O(1)$. J is the total angular momentum of the bound state. For the production at the LHC, one needs to include the integral of PDF in $\mathcal{L}_{q\bar{q}}$ with the center of mass energy set to the mass of the bound state.

III. HIGGSINO BOUND STATE IN λ-SUSY

A. Parameters in λ-SUSY

In λ-SUSY, a large value of λ helps to increase the Higgs mass to 125 GeV in a natural way [20]. The $\lambda S H_u H_d$ term in the superpotential induces the Yukawa coupling between Higgsinos/Singlino and the singlet scalar or Higgs boson, i.e.,

$$\mathcal{L} \supset \lambda\tilde{H}_u\tilde{H}_d s + \lambda\tilde{H}_u H_d\tilde{S} + \lambda H_u\tilde{H}_d\tilde{S} + \text{H.c.}, \tag{3}$$

where $\tilde{H}$ and $\tilde{S}$ are Higgsinos and Singlino. s is the scalar component of singlet S. Given that λ can be very large in

λ-SUSY, s can mediate a strong attractive force between Higgsinos. Once the Higgsinos are pair produced at the LHC, such a strong attractive force may induce a Higgsino bound state. The annihilation decay of this bound state may provide us a powerful handle on the search for Higgsinos.

Here, we study the parameter space in λ-SUSY, in which the neutralino bound state is important. Given the fact that s does not couple to Wino and Bino directly, we would like to focus on the scenario where the lightest neutralinos are mainly Higgsino and Singlino. Following the convention in [41], the general next to minimal supersymmetric standard model (NMSSM) superpotential is written as

$$W = \lambda S H_u H_d + \xi_F S + \frac{1}{2}\mu' S^2 + \frac{\kappa}{3} S^3. \tag{4}$$

In the Z_3 invariant NMSSM, ξ_F and μ' are absent. In the basis $\psi^0 = (-i\lambda_1, -i\lambda_2^3, \psi_d^0, \psi_u^0, \psi_S)$, the neutralino mass matrix is written as ($\mu_{\rm eff} = \lambda s$)

$$M_0 = \begin{pmatrix} M_1 & 0 & -\frac{g_1 v_d}{\sqrt{2}} & \frac{g_1 v_u}{\sqrt{2}} & 0 \\ & M_2 & \frac{g_2 v_d}{\sqrt{2}} & -\frac{g_2 v_u}{\sqrt{2}} & 0 \\ & & 0 & -\mu_{\rm eff} & -\lambda v_u \\ & & & 0 & -\lambda v_d \\ & & & & 2\kappa s + \mu' \end{pmatrix}. \tag{5}$$

If M_1 and M_2 are large compared to other parameters in the mass matrix, Wino and Bino are heavy, and their components in the lightest neutralino are negligible. The singlet scalar can couple to Higgsinos through a large Yukawa coupling λ or to Singlinos through a large κ term.

In principle, it is possible to form a bound state with an $O(1)$ mixing between Higgsino and Singlino. However, when the mixing is too large, it reduces the cross section of neutralino production because Singlino does not couple to the SM such as the W or Z boson. For simplicity, we assume $(2\kappa s + \mu') \gg \lambda v_{u,d}$ in order to decouple the Singlino component. We will see in later discussions that this limit is also helpful to relax the constraints from electroweak precision tests. Thus, in this case, the lightest neutralino states are mainly Higgsinos with a nearly degenerate spectrum. This guarantees the decay $\tilde{\chi}_2^0 \to \tilde{\chi}_1^0 +$ SM to be much slower than the annihilation decay of the bound state. Since the energy of bound state production is much larger than the splitting between two neutralinos, we can combine the neutalinos into a Dirac fermion and form an s-wave bound state through the vector coupling of Z. The singlet scalar s plays the role of force mediator binding the bound state. If we instead keep only one light neutralino, the Z-mediated bound state production of two Majorana fermions is p-wave suppressed.

Furthermore, when M_2 is very large, the lightest chargino is mainly a Higgsino, which is almost degenerate with the lightest neutralinos. A large value of λ also induces a large Yukawa coupling between the singlet and the charged Higgsinos, which allows the formation of bound states with two charginos or one chargino and one neutralino.

Finally, let us consider the mass matrix of CP-even scalar particles. Using the VEVs v_u, v_d, and $\langle s \rangle$ to eliminate several soft mass terms in the Lagrangian, the 3×3 mass matrix under the basis of (H_d, H_u, s) can be written as [42]

$$\begin{aligned} M_{11}^2 &= g^2 v_d^2 + (\mu_{\rm eff} B_{\rm eff} + \hat{m}_3^2) \tan\beta \\ M_{22}^2 &= g^2 v_u^2 + (\mu_{\rm eff} B_{\rm eff} + \hat{m}_3^2)/\tan\beta \\ M_{33}^2 &= \lambda(A_\lambda + \mu') \frac{v_u v_d}{\langle s \rangle} + \kappa \langle s \rangle (A_\kappa + 4\kappa \langle s \rangle + 3\mu') \\ &\quad - (\xi_S + \xi_F \mu')/\langle s \rangle \\ M_{12}^2 &= (2\lambda^2 - g^2) v_u v_d - \mu_{\rm eff} B_{\rm eff} - \hat{m}_3^2 \\ M_{13}^2 &= \lambda(2\mu_{\rm eff} v_d - (B_{\rm eff} + \kappa \langle s \rangle + \mu') v_u) \\ M_{23}^2 &= \lambda(2\mu_{\rm eff} v_u - (B_{\rm eff} + \kappa \langle s \rangle + \mu') v_d), \end{aligned} \tag{6}$$

where $g^2 = \frac{g_1^2 + g_2^2}{2}$, $B_{\rm eff} = A_\lambda + \kappa \langle s \rangle$, $\hat{m}_3^2 = m_3^2 + \lambda(\mu' \langle s \rangle + \xi_F)$, and m_3 A_λ, A_κ, ξ_S are the soft SUSY breaking parameters in a general NMSSM. It is quite involved to do a complete analysis on the possible parameter region. Here, we will only discuss the desired parametrization of this mass matrix for the bound state production and point out some subtleties of it.

First, let us rotate the mass matrix in Eq. (6) and study the physics in the basis (h_v^0, H_v^0, h_s^0) defined as

$$\begin{aligned} H_u^0 &= v_u + \frac{1}{\sqrt{2}}(\sin\beta h_v^0 + \cos\beta H_v^0), \\ H_d^0 &= v_d + \frac{1}{\sqrt{2}}(\cos\beta h_v^0 - \sin\beta H_v^0), \\ s &= \langle s \rangle + \frac{1}{\sqrt{2}} h_s^0. \end{aligned} \tag{7}$$

Only h_v^0 has tree level coupling with W and Z bosons under this basis. Given the fact that the lightest neutralino/chargino are dominantly Higgsinos, the most appealing scenario for the bound state production is the small mixing limit, where the singlet scalar only has a small mixing with other scalars. This is because a mixing in the singlet scalar will reduce its Yukawa coupling to Higgsinos. On the other hand, the mixing between h_v^0 and H_v^0 is strongly constrained by the LHC data while the mixing between h_v^0 and h_s^0 can be moderate [43].

This forces us to suppress all possible mixings in this mass matrix. However, when having no sizable mixing from other states, the tree-level mass of the SM-like Higgs can be approximated as

$$m_{h_v^0}^2 \sim \lambda^2 v^2 \sin^2 2\beta + m_Z^2 \cos^2 2\beta, \tag{8}$$

and if $\lambda \sim > 2$, the Higgs mass is too large when $\tan\beta \simeq 1$. If the singlet scalar is heavy, e.g., $m_s \simeq 400$ GeV, only a small mixing between (h_s^0, h_v^0) is required to drive the Higgs mass down, but then the Higgsino mass needs to be quite large ($m_{\tilde{\chi}} > 2m_s/\alpha_\lambda$) in order to form the bound state.

There are several ways to get around the above issues while having light Higgsinos bound state production. One is to consider the parameter region with $\tan\beta \sim > 5$, so the tree level mass of the SM-like Higgs is reduced. The model with a large $\tan\beta$ and $\lambda \sim 2$ can be highly constrained by EW precision tests (EWPT) [44]. There are three types of loop-contributions to the EWPT: Higgsino/Singlino, stop/sbottom, and CP-odd/-even Higgs bosons. In the Z_3 invariant version of NMSSM, contributions from the Higgsino loop diagrams can be significant at large $\tan\beta$. However, in a general NMSSM model, a larger μ' in Eq. (4) can raise the Singlino mass and suppress the Higgsino-Singlino mixing. This reduces the tension from EWPT. The contributions from the other two EWPT-violation channels are more moderate. In the Z_3-invariant NMSSM, the stop-sbottom contribution can be reduced by increasing the heavier charged Higgs mass $m_{H^\pm}$ [19]. Large soft masses of the stop and sbottom can also help to loosen the constraints, although a sizable tuning will be required. A large $m_{H^\pm}$ will also reduce constraints from the CP-odd/-even Higgs bosons, which are generally weaker in the Z_3-invariant NMSSM [44].

Besides having a larger $\tan\beta$, the other possibility to obtain the right Higgs mass and a light singlet scalar is to introduce another gauge singlet chiral supermultiplet, for example, $W \supset \lambda S H_u H_d + \mu S S'$. The scalar component s' can be heavy and play the role of lowering the SM-like Higgs mass to the observed value, while the singlet scalar s can be light and be the force mediator to form the Higgsino bound state [45].

Finally, we emphasize that in λ-SUSY, the coupling between H_u, H_d, and S is generically sizable. If the singlet mass is smaller than half the mass of the Higgs, it may induce a large decay branching ratio of $h \to ss$, unless properly tuning parameters to get a small coupling. Thus, we require s to be heavier than 62 GeV. On the other hand, s cannot be too heavy or else we cannot treat it as a light mediator to form the bound state of Higgsinos. This induces an upper limit for s mass, i.e., it should be smaller than the Bohr radius of the bound state $r_{\text{Bohr}} \sim \frac{2}{m_{\tilde{h}}\alpha_\lambda}$. Thus, we assume

$$\frac{m_h}{2} < m_s < \frac{m_{\tilde{h}}\alpha_\lambda}{2} \tag{9}$$

when calculating the bound state production.

B. Higgsinonium production

The bound state production is proportional to the wave function $|\psi(0)|^2$, and it is more plausible to discuss the s-wave ($\ell = 0$) state, which has a nonvanishing wave function at the origin. There are two s-wave bound states to be formed with two distinguishable fermions: 0^- and 1^- in the convention J^P for the spin (J) and parity (P). The pseudoscalar 0^- can be produced through a gluon fusion of the CP odd scalar in the complex scalar S, and the vector 1^- can be produced through the transverse component of the SM gauge bosons. Since the 0^- production depends on the details of the scalar spectrum, and the cross section from the loop-induced gluon fusion process is relatively small, we focus on the 1^- production in this work.

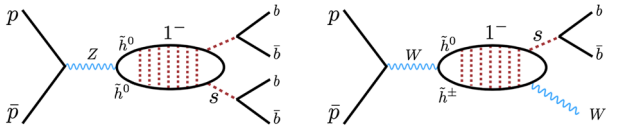

FIG. 1. Higgsinonium production and decay at the LHC.

The production of neutral bound state goes through the SM Z in Fig. 1 left.

$$q\bar{q} \to Z^* \to \tilde{h}\bar{\tilde{h}}\,. \tag{10}$$

The parton level amplitude from the vector mediation is written as

$$\mathcal{M}_{\tilde{h}\tilde{h}\to q\bar{q}} = \frac{g_{V\tilde{h}}}{q^2 - m_Z^2}(\bar{v}(k')\gamma^\mu u(k))(\bar{v}(p')\Gamma_\mu u(p)), \tag{11}$$

where $q^2 \simeq M^2 = (2m_{\tilde{h}})^2$ is the bound state mass, and (k', k) $((p', p))$ are the Higgsino (quark) momenta. The vector coupling of Higgsino has a coupling $g_{V\tilde{h}}$ and the latter forms a 1^- bound state, while the coupling between Z to quarks $\Gamma_\mu \equiv g_{Vq}\gamma_\mu + g_{Aq}\gamma^5\gamma_\mu$ carries both the vector and axial-vector components. Following the discussion in [38], we calculate the amplitude treating quarks in the relativistic limit. We sum the different spin configurations that match the total angular momentum $J = 1$ and take the average of the three 1^- polarizations for the bound state decay rate

$$\mathbf{\Gamma}_{\mathbf{1^-}\to q\bar{q}} = \frac{16\pi\alpha_{V\tilde{h}}(\alpha_{V\tilde{q}} + \alpha_{A\tilde{q}})|\psi(0)|^2 M^2}{(M^2 - m_Z^2)^2}, \tag{12}$$

where λ is the Yukawa coupling in Eq. (3). Using Eq. (2), we obtain the production cross section

$$\begin{aligned}\sigma^{NN}_{\mathbf{1^-}} &= \frac{\pi^2\zeta(3)\alpha_\lambda^3\alpha_{V\tilde{h}}(\alpha_{V\tilde{q}} + \alpha_{A\tilde{q}})M^4}{3s(M^2 - m_Z^2)^2}\mathcal{L}_{q\bar{q}} \\ &= \frac{\pi^2\zeta(3)\alpha_\lambda^3\alpha_{Z\tilde{h}}M^4}{3s(M^2 - m_Z^2)^2} \\ &\quad \times \left[\sum_q \alpha_{Zq_{V,A}}\int_{M^2/s}^1 \frac{dx}{x} f_q(x) f_{\bar{q}}\left(\frac{M^2}{xs}\right) + (q \leftrightarrow \bar{q})\right].\end{aligned} \tag{13}$$

The result also includes the color factor $N_c = 3$. The production cross sections at the 13 TeV LHC and

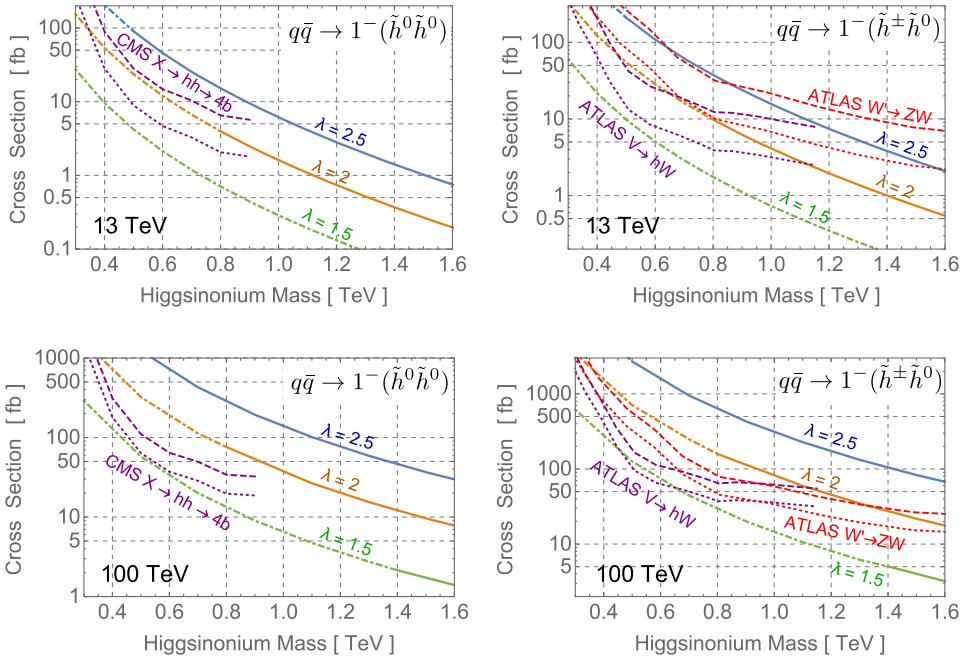

FIG. 2. Upper left: Higgsinonium production through $pp \to Z^* \to (\tilde{h}^0\bar{\tilde{h}}^0)$ into 1^- bound state under different assumptions of the λ coupling. The solid curves show production cross sections in which a nonvanishing mass window Eq. (9) of the singlet scalar exists. The dash-dotted extension of the curves has $m_s < m_h/2$, which violates the invisible Higgs decay constraint unless a tuned coupling or an extra singlet field is included. The purple dashed (dot-dashed) curves show the 13 TeV projection of the CMS resonance search $pp \to X \to hh \to 4b$ [47] with 300 fb^{-1} (3 ab^{-1}) of data. The bound gives an idea of the possible future reach if the singlet scalar has a similar mass and decay branching ratio to the SM Higgs. Upper right: the production $q\bar{q} \to W^* \to (\tilde{h}^\pm\tilde{h}^0)$ into the 1^- state. The purple dashed (dotted) curve shows the 13 TeV projection of the ATLAS resonance search $pp \to V \to Wh$ [48] with 300 fb^{-1} (3 ab^{-1}) of data. The red dashed (dotted) curve shows the 13 TeV projection of the ATLAS search $pp \to W' \to WZ$ [49] with 300 fb^{-1} (3 ab^{-1}) of data, with the Z branching ratio rescaled to the singlet scalar into $b\bar{b}$. The ZW bound can be used to compare with the scenario when the singlet mass similar to Z, and the efficiency of the $Z \to$ jets tagging is similar for the singlet scalar decay. Lower plots: the same plots for a 100 TeV hadron collider. The dashed (dotted) curves correspond to projections for 1 ab^{-1} (3 ab^{-1}) of data.

100 TeV collider are shown in Fig. 2 (left). Comparing to the Higgsino production rate at the LHC, there is ~20% probability that the produced Higgsinos form a 1^- bound state when $\lambda = 2$.

For the charged and neutral Higgsino production (Fig. 1 right),

$$pp \to W^{\pm *} \to \tilde{h}^0\tilde{h}^\pm, \tag{14}$$

the electrically charged 1^- state is produced with a cross section

$$\sigma^{NC}_{\mathbf{1}^-} = \frac{\pi^2\zeta(3)\alpha_\lambda^3\alpha_W^2}{3s}\frac{M^4}{(M^2-m_W^2)^2} \times \left[\sum_q \int_{M^2/s}^1 \frac{dx}{x} f_{q_u}(x) f_{\bar{q}_d}\left(\frac{M^2}{xs}\right) + (q_u \leftrightarrow \bar{q}_d)\right]. \tag{15}$$

The result is shown in Fig. 2 (right) for the 13 TeV LHC and the 100 TeV collider. Comparing to the total production of the neutral and charged Higgsinos, about 20% of the events will form the 1^- bound state.

C. Annihilation decay channels

Here, we consider the possible decay channels of the bound states [50]. Let us first consider the bound state formed by two neutralinos. As discussed previously, the singlet scalar s needs to be much lighter than $m_{\tilde{\chi}}$. Since λ is large, the annihilation is dominantly to two s scalars. The singlet scalar generically mixes with the Higgs. If its mass is small, its dominant decay channel is to b quarks. If s is heavier than 140 GeV, which means the Higgsino bound states are very heavy according to Eq. (9), the dominant decay is through the diboson channel. Similar arguments can be applied to the neutral bound state formed by two charginos. Thus, for small m_s, the dominant search channel is 4 b-jet events with two paired resonance, and 4 b jets together form a resonance of the bound state. For a heavier s, the dominant channel is the 4-boson event with two paired resonances, also with a heavier resonance from all objects.

It is important to know whether the heavy resonance is too broad to search at the LHC. To estimate the width of the bound state, we approximate the scattering matrix of two stationary neutralinos annihilating to two scalars

$$|\mathcal{M}(2\tilde{N} \to 2s)|^2 \sim \lambda^4 \tag{16}$$

by assuming m_ϕ to be much smaller than the typical energy scale of the process, which is the mass of the bound state. Also, we drop all angular dependencies since they only contribute as $O(1)$ corrections after phase space integral. In order to convert this 2-to-2 scattering matrix to the width of the bound state, we need to combine $|\mathcal{M}(2\tilde{N} \to 2s)|^2$ with the wave function, which gives

$$\Gamma(B \to 2s) \sim \frac{\lambda^4}{\pi}\frac{|\psi(0)|^2}{M_B^2} \sim \frac{\alpha_\lambda^5}{4} M_B. \tag{17}$$

Now we see that the width of the bound state can be much smaller than the mass of the bound state. For example, if the bound state is 1 TeV with $\lambda = 2$, the width is $\simeq$1 GeV. Thus, we can safely treat the heavy resonance as a narrow width particle as long as λ is not too big.

To estimate how well future resonance searches can constrain the annihilation decay, we adopt the bound from the CMS search of a heavy resonance X decaying into $hh \to 4b$'s [47] by focusing on the case when the singlet scalar has a similar mass and decay branching ratio to the SM Higgs. To compare to bounds with future searches, we rescale the expected cross section bound from the existing 8 TeV search according to the parton distribution function (PDF). We describe the details in the Appendix. Projecting the search to the 13 TeV search with 300 fb^{-1} (3 ab^{-1}) of data, the upper bound on the resonance search with 95% C.L. is shown in the purple dashed (dotted) curve in the upper left plot in Fig. 2. Even with no further improvement on the search designed for the scalars, our projection has shown the possibility of reaching the bound state with $\lambda = 2$ coupling. The bounds are only applied to $M < 900$ GeV due to the kinematic limit in the 8 TeV search. Higher mass bins lack statistics, and our simple $\sqrt{N}$ rescaling of the uncertainty may fail. For the future projection, the bound for mass above 900 GeV should be better than the lower mass region. We leave careful study of collider constraints for future work.

Compared to the neutralino-neutralino or chargino-chargino pair production, the cross section of the chargino-neutralino pair production at 13 TeV is about 5 times larger when $m_{\tilde{h}} > 400$ GeV. Beside the larger production cross section, the annihilation channel for the charged bound state is also different from the neutral bound state. Due to charge conservation, the dominant decay channel is $(W^\pm + s)$. Thus, the dominant signal channel is either $(W^\pm + 2b)$ or 3-boson, depending on m_s. Similar to the neutral bound state scenario, there can be a heavy resonance. Compared to the neutral bound state case, the width of the charged bound state is smaller because at one of the coupling vertices λ is replaced by the $W^\pm$ coupling.

Similar to the neutral bound state, we show a projection of the ATLAS vector resonance search $V \to Wh$ [48] at 13 TeV with 300 fb^{-1} (3 ab^{-1}) in the red dashed (dotted) curve of Fig. 2 (right), assuming the singlet scalar has the same mass and decay branching ratios as the SM Higgs. To cover the higher mass region, we also show the projected bound on the $W' \to WZ \to \ell\nu jj$ search at ATLAS [49] in the purple dashed (dotted) curve for 13 TeV with 300 fb^{-1} (3 ab^{-1}) of data by rescaling the $Z \to$ jets branching ratio into the singlet to $b\bar{b}$. If the tagging efficiencies between the s and Z are not too different, these curves give an estimate of the future search reach.

It is interesting to compare the reach of the Higgsinonium search to the typical missing energy study. In [51], the authors estimate the future bound on the Higgsino mass from the monojet + MET search, assuming the Higgsino to be the lightest SUSY particle. The 95% C.L. constraint from the 14 TeV study with 3 ab^{-1} of data is $m_{\tilde{h}} \gtrsim 200$ GeV, and from the 100 TeV collider is $m_{\tilde{h}} \sim > 700$ GeV. When $\lambda \sim > 2$, our bounds in Fig. 2 can be better than these results.

IV. THE SIDM BOUND STATE

The bound state annihilation decay may also exist in DM models with a strong self-interaction. An important motivation for the SIDM model is the possibility of solving anomalies in small scale structures, including the too big to fail problem and the disagreement of the core/cusp halo structure obtained between observation and N-body simulations [13–16]. When considering the structure of dwarf DM halos, the self-interaction with $\sigma_T/m_\chi \sim 0.5$–50 cm$^2/g$ on dwarf scales can produce smooth core density in dwarf galaxies in accordance with observations [52,53].

In this work, we consider light mediator models that can generate a cross section favored by DM profile measurements in dwarf galaxies. We study the annihilation decay of the SIDM particles at colliders. We assume DM, χ, is fermionic. Its self-interaction is induced by a light scalar mediator ϕ through the Yukawa coupling $\lambda_\chi \bar{\chi}\phi\chi$ + H.c., or a vector mediator A' through a gauge coupling $-i\lambda_\chi \bar{\chi}A'\chi$. The self-scattering $\chi\bar{\chi} \to \chi\bar{\chi}$ has a t-channel enhancement in the nonrelativistic limit when mediator mass is lower than the momentum transfer.

In order to form DM bound states at colliders, we need the mediator wavelength to be longer than the Bohr radius, $\alpha_\chi m_\chi/m_{\rm med} \gtrsim 2$ ($\alpha_\chi \equiv \lambda_\chi^2/4\pi$). Born approximation does not apply to DM self-scattering any more when $\alpha_\chi m_\chi/m_{\rm med} \gtrsim 1$. Thus, we have to take into consideration nonperturbative effects.

Further, as we will discuss in a later section, if $m_{\rm med} \ll 10$ MeV, the decay length of the mediators from the DM annihilation is generically too long for collider searches. We thus limit the discussion to mediator masses $m_{\rm med} \gtrsim 10$ MeV. DM particles with mass around $\mathcal{O}$(1–100) GeV is our focus from a collider point of view; thus, we have $m_\chi v/m_{\rm med} \lesssim 1$, where $v \sim 10^{-4}$ is the viral

velocity of dwarf galaxies. Under this choice of parameters, quasibound states of DM can form, in which case, the quantum mechanical resonances and antiresonances emerge for the SIDM interaction. The analytical approximation obtained in this regime is written as (for the full expression, please see [16])

$$\sigma_T = \frac{16\pi}{m_\chi^2 v^2}\sin^2\delta_0. \tag{18}$$

For an attractive force, the resonance effect makes $\sin\delta_0 \to 1$ when $\alpha_\chi m_\chi/1.6m_{\rm med} = n^2$, $n = 1, 2, 3, \ldots$ in the small velocity limit. On the other hand, antiresonance, with vanishing s-wave cross section, happens when $\sin\delta_0 \to 0$, i.e., $n \approx 1.69, 2.75, 3.78, \ldots$. If the force is repulsive, which happens in an asymmetric DM model with a dark photon mediator, there is no resonance or antiresonance effect, and the cross section is calculated by the full expression in Eq. (18). For the DM mass and couplings we study below, the self-interacting cross section satisfies the bullet cluster and cluster shape constraints with the typical velocity $v \sim 10^{-2}$ and $\sigma_T/m_\chi \lesssim 1\ {\rm cm}^2/g$ [53,54].

For a given value of (m_χ, α_χ), we can obtain the mediator mass $m_{\rm med}$ that gives the right scattering cross section ($0.550\ {\rm cm}^2/{\rm g}$) by solving Eq. (18). The solution is not unique due to the finite range of the scattering cross section and the resonance/antiresonance behavior in the attractive case. When the m_χ is heavy (light), the solution of the mediator mass in the attractive case is closer to the (anti) resonance region. We make sure the mediator mass as the solution also satisfies $m_{\rm med} < \alpha_\chi m_\chi/2$ required by the bound state production. In the following study, we make sure each choice of (m_χ, α_χ) has a corresponding $m_{\rm med}$ satisfying the above constraints. However, since the bound state production is insensitive to the mediator mass, we keep the value of $m_{\rm med}$ implicit when showing the results.

In a thermal relic DM scenario, the size of α_χ has an upper bound from the DM density, which limits the collider production of the DM bound states. However, as this bound can be avoided in various scenarios, such as the context of asymmetric DM or nonthermal production, we will not take it into account for the study.

A. Darkonium production

In order to study the bound state production rate, we parametrize the DM-SM interaction by effective operators

$$0^-: \frac{m_q(\bar{q}\gamma^5 q)(\bar{\chi}\gamma^5\chi)}{v_h M_*^2}, \qquad 1^-: \frac{(\bar{q}\gamma^\mu\gamma^5 q)(\bar{\chi}\gamma_\mu\chi)}{M_*^2}. \tag{19}$$

Here, $v_h = 174$ GeV, and the quark mass in the pseudoscalar coupling can come from a straightforward UV completion in which the chiral symmetry breaking induces a Yukawa coupling insertion. The γ^5 in the vector mediation causes velocity suppression in DM direct detection experiments. Also, the scattering with DM and nucleus is spin-dependent. Thus, this operator is less constrained. In contrast to the missing energy search at high energy colliders, the use of effective operators in bound state production is well justified. The center of mass energy is fixed to be around $2m_\chi$. This is much lower than $4\pi M_*$, which can be probed in collider searches.

For the 0^- state from the quark production, the decay rate from the bound state into quarks is written as

$$\Gamma_{0^-\to q\bar{q}} = \frac{3}{\pi M^2}\left(\frac{M}{M_*}\right)^4\left(\frac{m_q}{v_h}\right)^2|\psi(0)|^2, \tag{20}$$

where M is the mass of the bound state. The result includes a color factor and a summation of the correct spin configurations that match the $J = 0$ state. Using Eq. (2), the production cross section is written as

$$\sigma_{0^-} = \frac{\zeta(3)\alpha_\chi^3}{48s}\left(\frac{M}{M_*}\right)^4 \times\left[\sum_q\left(\frac{m_q}{v_h}\right)^2\int_{M^2/s}^1\frac{dx}{x}f_q(x)f_{\bar{q}}\left(\frac{M^2}{xs}\right) + (q\leftrightarrow\bar{q})\right]. \tag{21}$$

In Fig. 4, we show the region of mediation scale M_* that gives at least 1 fb bound state production rate with different choices of the SIDM coupling. The smaller M_* region is excluded by the ATLAS heavy quark search at the LHC run 1. For this operator, the b-quark dominates the production. When the center of mass energy is larger for heavier DM production, b-quark PDF decreases faster compared to that of light quarks. This makes the bound on 0^- weaken faster than the production channels, which are dominantly through light quarks, e.g., 1^- as discussed later. We require $\alpha_\chi < 1$ for the perturbation calculation, which implies that the parton in the bound state is nonrelativistic.

Similar to the Higgsino case, the bound state production of 1^- through the axial-vector mediated process can be obtained by Eq. (13) with $g_V = 1$ and $M_V = M_* \gg M$

$$\sigma_{1^-} = \frac{\zeta(3)\alpha_\chi^3}{48\,s}\left(\frac{M}{M_*}\right)^4 \times\left[\sum_q\int_{M^2/s}^1\frac{dx}{x}f_q(x)f_{\bar{q}}\left(\frac{M^2}{xs}\right) + (q\leftrightarrow\bar{q})\right]. \tag{22}$$

In the right plot of Fig. 4, we show the region of mediation scale M_* which gives at least 1 fb bound state production cross section with various choices of the SIDM coupling.

B. Annihilation decay channels

With large self couplings, the SIDM bound states prefer to decay into light mediators rather than the SM quarks. Instead of surveying a comprehensive list of possible

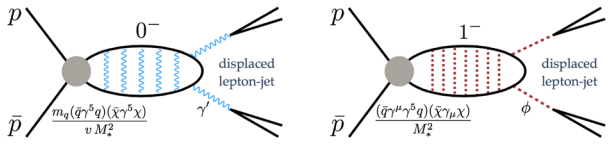

FIG. 3. Darkonium production and decay at the LHC.

mediators, we focus on a few illustrative examples. For vector bound state 1^-, we consider the case where the mediator is a scalar. The decay of the bound state into two light scalars can be characterized by a derivative coupling $V^{\mu}_{1^-}\phi^* i\overleftrightarrow{\partial_\mu}\phi$ [55]. This decay rate is of order $\sim\alpha_\chi^5 M/8\pi$, which gives a prompt $1^- \to \phi\phi^*$ decay.

Generically, the force mediators are not stabilized by a symmetry (for exceptions, see [56,57]) and can decay into SM particles. For the scalar mediator ϕ, we parametrize the decay using the effective coupling $\hat{y}_{ij}\phi\bar{L}_i H E_j/\Lambda \supset \epsilon_{\phi,ij}\phi\bar{\ell}_i\ell_j$, where $\hat{y}_{ij}$ is aligned to the SM Yukawa coupling. The scalar can also couple to SM through the Higgs mixing, but the coupling is generically more suppressed due to constraints from the Higgs coupling measurement [58], as well as the small Yukawa coupling to the light SM fermions. If the effective coupling is generated by an electroweak (EW) scale mediation, and $\hat{y}_{ij}$ is indeed the SM Yukawa coupling, $\epsilon_{\phi,ee}$ can be as small as $O(10^{-6})$. Figure 3 (left) shows the production and decay of the bound state.

On the other hand, we assume the 0^- bound state decays into dark photons. The decay of 0^- can be described by a pseudoscalar coupling $\frac{i}{\Lambda}a_{0^-}F'_{\mu\nu}\tilde{F}'^{\mu\nu}$. In the microscopic picture, the annihilation $\chi\bar{\chi}\to\gamma'\gamma'$ that generates the $F'_{\mu\nu}\tilde{F}'^{\mu\nu}$ interaction needs to break the parity. This requires the dark photon to couple chirally to the DM fermions. Further, dark photons decay to SM through kinetic mixing $\epsilon_{\gamma'}F_{\mu\nu}F'^{\mu\nu}$ to the normal photon. Currently, the bound from the various dark photon searches requires $\epsilon_{\gamma'}\lesssim 10^{-3}$ for $m_{\gamma'} > 10$ MeV [63]. We will study the γ' decay with a mixing satisfying the bound. Figure 3 (right) shows the production and decay of the bound state.

We focus on the mediator decay into e^+e^-. As heavier mediators open up other decay channels such as muon and pion, we leave a more complete analysis for future work. The two types of mediator decay have lengths

$$c\tau_{\phi\to e^+e^-} \simeq \gamma_\phi\left(\frac{\epsilon_\phi^2 m_\phi}{8\pi}\right)^{-1} \simeq 5\text{ cm}\times\gamma_\phi\left(\frac{100\text{ MeV}}{m_\phi}\right)\left(\frac{10^{-6}}{\epsilon_\phi}\right)^2, \quad (23)$$

$$c\tau_{\gamma'\to e^+e^-} \simeq \gamma_{\gamma'}\left(\frac{e^2\epsilon_{\gamma'}^2 m_{\gamma'}}{12\pi}\right)^{-1} \simeq 0.08\text{ mm}\times\gamma_{\gamma'}\left(\frac{100\text{ MeV}}{m_{\gamma'}}\right)\left(\frac{10^{-4}}{\epsilon_{\gamma'}}\right)^2. \quad (24)$$

The boost factor $\gamma_{\phi,\gamma'}\simeq m_\chi/m_{\phi,\gamma'}$ can be larger than 10^2, which provides a good chance to observe displaced decays. However, the large boost also corresponds to a small opening angle between e^+e^-, which makes searches relying on reconstructing the displaced vertices (DV) difficult. Even if the magnetic field can eventually open up the e^+e^- angle, multiscatterings of the e^+e^- inside the tracker and electromagnetic calorimeter (ECAL) can still limit the precision. Further study including the detector performance is then necessary for the standard DV search.

One displaced search that cares less about opening angle is the displaced lepton jet (DLJ) search. When the decay length is long enough, a sizable fraction of the decays can

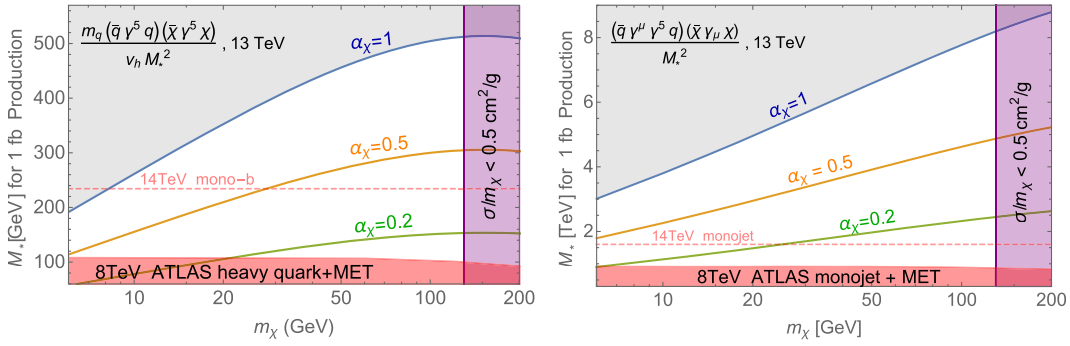

FIG. 4. Left: the mediation scale M_* for having a 1 fb 0^- bound state production through the pseudoscalar mediation at 13 TeV LHC. The red-shaded region shows the 95% C.L. exclusion bound from the 8 TeV ATLAS heavy quark + MET search [59]. The dashed curve shows the 95% C.L. bound from the mono-b search estimated in [60], assuming 300 fb^{-1} of data at 14 TeV LHC. The purple-shaded region has the DM scattering $\sigma/m_\chi < 0.5$ cm$/g^2$ at dwarf galaxies (assume $v = 10^{-4}$), assuming $m_{\rm med}$ matches the size of (m_χ, α_χ) that gives $\sin\delta_0 = 1$ in Eq. (18). The gray-shaded region corresponds to $\alpha_\chi > 1$, for which the nonrelativistic calculation of the bound state production fails. Right: the 1 fb region of the 1^- state through the vector coupling. The red-shaded region corresponds to the 95% C.L. exclusion bound from the 8 TeV ATLAS monojet search [61]. The dashed curve shows the 95% C.L. bound from the monojet search estimated in [62], assuming 300 fb^{-1} of data at 14 TeV LHC.

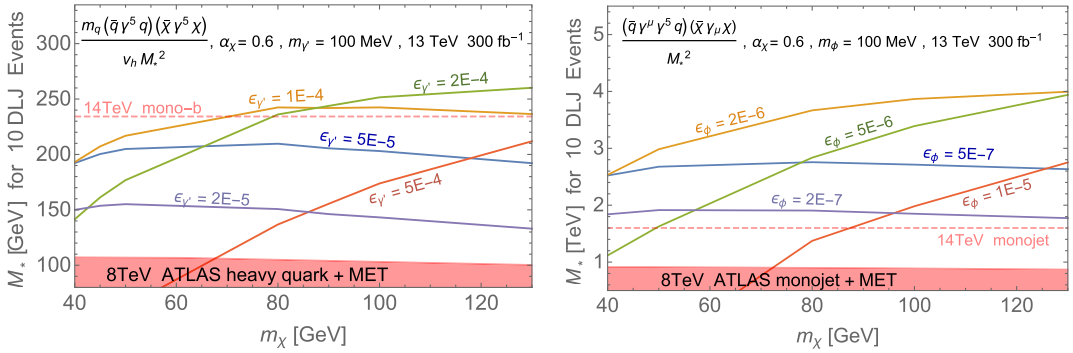

FIG. 5. Left: the mediation scale M_* of the pseudoscalar operator for the 0^- bound state production. The 0^- decays into two dark photons, which have displaced decays into e^+e^- and form displaced lepton jet (DLJ) signals. The light mediator mass is fixed to be $m_{\rm med} = 100$ MeV, and different curves correspond to different sizes of the mixing $\epsilon_{\gamma'} F_{\mu\nu} F'^{\mu\nu}$. We require 10 events containing two identified DLJ's at the HCAL from the dark photon decay, assuming 300 fb^{-1} of data at 13 TeV LHC. See details in the text for the assumed cuts and reconstruction efficiency. Right: the mediation scale M_* of the axial-vector operator for the 1^- bound state production. The 1^- decays into two scalar mediators, which have displaced decays into e^+e^- and give the DLJ signals. Different curves correspond to different sizes of the coupling $\epsilon_\phi \phi \bar{e} e$. The current and projected bounds from the missing energy searches are described in Fig. 4. Two remarks: first, compared to the bound state production rate in Fig. 4, the signal efficiency of our DLJ study is of order 0.1%–1%. A better searching strategy, such as including signals in the tracker and μ chamber, may improve the result. Moreover, the M_* bound from the mono-b search is much lower than the typical center of mass energy at 14 TeV LHC. Therefore, simplified models with light mediators will give more accurate descriptions of collider signal, and the result will depend on the assumption of mediator coupling. Here, we include results from effective operators to show an estimated mediation scale that the missing energy searches can reach.

happen in the HCAL, making a "jet" that does not show up in the ECAL and the tracker.

To estimate the bounds on the DM bound state production, we adopt the cuts used in the 8 TeV ATLAS search for the displaced LJ [64] by requiring two e^+e^- jets produced in the HCAL with $2.0 < r_{\rm DLJ} < 3.6$ m, $\Delta R(e^+, e^-) \leq 0.5$, $p_T({\rm LJ}) > 30$ GeV, and $|\eta(\ell)| < 2.5$. We carry out our simulation at the 13 TeV LHC with 300 fb^{-1} of data. Beside the cuts, a 25% reconstruction efficiency for identifying both lepton jets is multiplied to get the number of signal events. This number is close to the efficiency obtained in the ATLAS study. In contrast to the dark photon search in [64], we can further require the total invariant mass of the DLJ's to be near the DM bound state mass, which will further reduce the SM background dominated by the multijets and cosmic ray events.

In Fig. 5, we show the estimated lower bounds on the mediation scales in the effective operators of 0^- and 1^- production, assuming the exclusion bound requires less than 10 observed events with $m_{\phi,\gamma'} = 100$ MeV. The bound is obtained by a parton level study using MadGraph 5[65] and model generator Feynrules 2.3 [66]. In order to capture the correct energy and angular distribution of the light mediators, we use the effective coupling $aF'_{\mu\nu}\tilde{F}'^{\mu\nu}/\Lambda'$ to describe the 0^- decay into dark photons, and $\lambda_\chi V_\mu \phi^* \partial^\mu \phi$ for the 1^- decay into scalars. The decay probability within a given decay length is calculated using the events passing the energy and angular cuts. As one can see, the displaced LJ search can explore a wide range of currently unconstrained mediation scales. When the mixing angle is small (the purple, blue curves), the mediator tends to decay outside the collider. Bounds on a lighter DM is then stronger because it gives a smaller boost to the mediators. On the other hand, with a larger mixing (the green, red curves), the meditator tends to decay before it reaches ECAL. Thus, a heavier DM is more constrained.

V. SUMMARY

In this paper, we study the collider physics of bound state production of strongly coupled particle pairs. Such scenarios are well motivated by the large Yukawa coupling mediated by gauge singlet or Higgs boson in λ-SUSY, as well as the self-interacting dark matter scenario.

In λ-SUSY, the large value of λ introduces a sizable Yukawa coupling. The pair produced neutralino/chargino at the LHC can form a bound state by exchanging singlet/Higgs. The annihilation decay final states of neutralino pair or chargino pair are dominantly the scalar mediator. If the scalar mediator is lighter than 140 GeV, the dominant search channel is 4-b jets. These four b jets pair up to form two lighter peaks, and all four b jets form a heavier resonance. Otherwise, the final state has 4 W bosons if both mediator and Higgsino are heavy. On the other hand, the bound state formed by chargino and neutralino dominantly decay to one W boson and one scalar mediator. When the mediator is light, one can look for $2b + 1l +$ MET or boosted hadronic W and 2 b jets. This particular channel has not been studied in detail. If the mediator is heavy, the final state has 3 W bosons. In order to estimate the reach, we rescale the result of a heavy vector boson search at 8 TeV with respect to parton luminosity. Note that this rescaling procedure is only valid when statistical error dominates and the number of events is large in the relevant

bins. Thus, this estimate is only valid when the bound state mass is below TeV. If the bound state is very heavy, the number of events in the high energy bins is quite small. A naive rescaling tends to give a too conservative result. A more careful collider physics search is necessary in order to get a more precise estimation. With the conservative estimation we carry out, we find the 13 TeV LHC running can already probe interesting regions of λ-SUSY, $\lambda \simeq 2$. The reach can be further improved at a 100 TeV machine.

In SIDM, the DM self-interaction may be explained by a light force mediator strongly coupled to DM particles. The bound state of DM can be formed at the collider by exchanging the light force mediator. The annihilation decay of this DM bound state will dominantly produce two highly boosted mediators. The decay of the mediator can be either prompt or displaced, depending on how it mixes with the SM sector and how strong the mixing is. If the decay is prompt, one needs to look for the signature of a double bump that further reconstructs a heavier resonance. If the decay is displaced, the signature is more spectacular and the SM background is very small. Compared to various mono-X + MET searches, forming bound states provides much easier access to new physics and allows mass measurements of particles in the dark sector. We have shown that the sensitivity from the LHC can go well beyond the reach of monojet searches. Further, it is more proper to use the language of effective operators to describe DM production in the bound state scenario than the monojet scenario. The typical energy of the bound state production process is fixed to be the mass of the bound state, which is usually below the mediation scale that one constrains. The validity of using an effective operator description reduces subtleties on the conclusion one can draw from mono-X searches.

ACKNOWLEDGMENTS

We are grateful to Guido Ciapetti and Hai-Bo Yu for useful discussions. We also thank Bibhushan Shakya for reading the draft and give important comments. Y. T. is supported by the National Science Foundation Grant No. PHY-1315155 and by the Maryland Center for Fundamental Physics. L. W. is supported in part by the Kavli Institute for Cosmological Physics at the University of Chicago through Grant No. NSF PHY-1125897 and an endowment from the Kavli Foundation and its founder Fred Kavli. Y. Z. is supported by Grant No. DE-SC0007859. We thank Bibhushan Shakya for very helpful discussions on the NMSSM mass spectrum.

APPENDIX: PROJECTION OF FUTURE SEARCHES

Here, we discuss the projection of the 8 TeV vector resonance search to the 13 TeV LHC, following the concepts described in [67]. The significance of a resonance search is dominated by the number of signals versus the background near the resonance peak. Since the number of events in a hadron machine is dominated by the PDF, we can project the future bound by rescaling the PDF at a higher energy. Taking the current cross section constraints of the new signal as a function of the invariant mass, $\sigma_S^8(M)$, we obtain the bound at 13 TeV by solving

$$\frac{\sigma_S^8(M)L_8}{\sqrt{(\sigma_B^8(M)L_8\epsilon_8)^2+\sigma_B^8(M)L_8}} = \frac{\sigma_S^{13}(M)L_{13}}{\sqrt{(\sigma_B^{13}(M)L_{13}\epsilon_{13})^2+\sigma_B^{13}(M)L_{13}}}. \quad \text{(A1)}$$

Here, $L_{8,13}$ are the integrated luminosity at the 8 and 13 TeV searches. $\sigma_B^{8,13}(M)$ is the SM background near the resonance peak, which we assume to be rescaled by the PDF with

$$\sigma_B^8(M)/\sigma_B^{13}(M) \sim \mathcal{L}_{ij}(M,s_8)/\mathcal{L}_{ij}(M,s_{13}),$$
$$\mathcal{L}_{ij} = \frac{M^2}{s}\int_{M^2/s}^1 \frac{dx}{x} f_i(x) f_j\left(\frac{M^2}{xs}\right). \quad \text{(A2)}$$

Assuming the percentage systematic uncertainty ϵ_{13} at 13 TeV will be scaled down by the increasing statistics of the relevant control sample events, $\epsilon_{13} \approx \epsilon_8\sqrt{\sigma_B^8(M)L_8/\sigma_B^{13}(M)L_{13}}$, the projected bound is written into

$$\sigma_S^{13}(M) \approx \sqrt{\frac{L_8}{L_{13}}}\sqrt{\frac{\sigma_B^{13}(M)}{\sigma_B^8(M)}}\sigma_S^8(M). \quad \text{(A3)}$$

In more detail:

(i) CMS $X \to hh \to 4b$ [47]: the 8 TeV search uses 17.9 fb^{-1} of data, with the dominant background given by the multijet events. We use the gluon PDF to rescale the background cross section.

(ii) ATLAS $V \to Wh \to \ell\nu b\bar{b}$ [48]: the 8 TeV search uses 20.3 fb^{-1} of data, with the dominant background given by $t\bar{t}$. We use the gluon PDF to rescale the background cross section.

(iii) ATLAS $W' \to WZ \to \ell\nu jj$ [49]: the 8 TeV search uses 20.3 fb^{-1} of data, with the dominant background given by the W + jets events. We use the quark PDF to rescale the background cross section. We also multiply the branching ratio of $Z \to$ jets into the result and reproduce the actual cross section being constrained in the search.

[1] A. Birkedal, K. Matchev, and M. Perelstein, Phys. Rev. D **70**, 077701 (2004).
[2] Y. Bai, P. J. Fox, and R. Harnik, J. High Energy Phys. 12 (2010) 048.
[3] J. Goodman, M. Ibe, A. Rajaraman, W. Shepherd, T. M. P. Tait, and H.-B. Yu, Phys. Rev. D **82**, 116010 (2010).
[4] H. An, B. Echenard, M. Pospelov, and Y. Zhang, arXiv: 1510.05020.
[5] H. An, R. Huo, and L.-T. Wang, Phys. Dark Univ. **2**, 50 (2013).
[6] Y. Bai and J. Berger, J. High Energy Phys. 11 (2013) 171.
[7] J. Liu, B. Shuve, N. Weiner, and I. Yavin, J. High Energy Phys. 07 (2013) 144.
[8] D. N. Spergel and P. J. Steinhardt, Phys. Rev. Lett. **84**, 3760 (2000).
[9] S.-H. Oh, W. J. G. de Blok, E. Brinks, F. Walter, and R. C. Kennicutt, Jr., Astron. J. **141**, 193 (2011).
[10] M. Boylan-Kolchin, J. S. Bullock, and M. Kaplinghat, Mon. Not. R. Astron. Soc. **415**, L40 (2011).
[11] M. Boylan-Kolchin, J. S. Bullock, and M. Kaplinghat, Mon. Not. R. Astron. Soc. **422**, 1203 (2012).
[12] M. G. Walker and J. Peñarrubia, Astrophys. J. **742**, 20 (2011).
[13] M. Vogelsberger, J. Zavala, and A. Loeb, Mon. Not. R. Astron. Soc. **423**, 3740 (2012).
[14] M. Rocha, A. H. G. Peter, J. S. Bullock, M. Kaplinghat, S. Garrison-Kimmel, J. Oñorbe, and L. A. Moustakas, Mon. Not. R. Astron. Soc. **430**, 81 (2013).
[15] J. Zavala, M. Vogelsberger, and M. G. Walker, Mon. Not. R. Astron. Soc. **431**, L20 (2013).
[16] S. Tulin, H.-B. Yu, and K. M. Zurek, Phys. Rev. D **87**, 115007 (2013).
[17] G. Aad *et al.* (ATLAS Collaboration), Phys. Lett. B **716**, 1 (2012).
[18] S. Chatrchyan *et al.* (CMS Collaboration), Phys. Lett. B **716**, 30 (2012).
[19] R. Barbieri, L. J. Hall, Y. Nomura, and V. S. Rychkov, Phys. Rev. D **75**, 035007 (2007).
[20] L. J. Hall, D. Pinner, and J. T. Ruderman, J. High Energy Phys. 04 (2012) 131 (2012).
[21] The name Darkonium in the DM context was first used in [22] for a stable DM bound state in an asymmetric DM model. Weakly coupled DM bound states have been studied in [23–27].
[22] R. Laha, Phys. Rev. D **92**, 083509 (2015).
[23] M. Pospelov and A. Ritz, Phys. Lett. B **671**, 391 (2009).
[24] J. D. March-Russell and S. M. West, Phys. Lett. B **676**, 133 (2009).
[25] D. E. Kaplan, G. Z. Krnjaic, K. R. Rehermann, and C. M. Wells, J. Cosmol. Astropart. Phys. 05 (2010) 021.
[26] E. Braaten and H. W. Hammer, Phys. Rev. D **88**, 063511 (2013).
[27] M. B. Wise and Y. Zhang, Phys. Rev. D **90**, 055030 (2014); **91**, 039907(E) (2015).
[28] M. Beltran, D. Hooper, E. W. Kolb, Z. A. C. Krusberg, and T. M. P. Tait, J. High Energy Phys. 09 (2010) 037.
[29] P. J. Fox, R. Harnik, J. Kopp, and Y. Tsai, Phys. Rev. D **84**, 014028 (2011).
[30] P. J. Fox, R. Harnik, J. Kopp, and Y. Tsai, Phys. Rev. D **85**, 056011 (2012).
[31] A. Rajaraman, W. Shepherd, T. M. P. Tait, and A. M. Wijangco, Phys. Rev. D **84**, 095013 (2011).
[32] L. M. Carpenter, A. Nelson, C. Shimmin, T. M. P. Tait, and D. Whiteson, Phys. Rev. D **87**, 074005 (2013).
[33] T. Lin, E. W. Kolb, and L.-T. Wang, Phys. Rev. D **88**, 063510 (2013).
[34] Also see [4,35,36] for another example of producing mediators from the DM production.
[35] A. Gupta, R. Primulando, and P. Saraswat, J. High Energy Phys. 09 (2015) 079.
[36] M. Buschmann, J. Kopp, J. Liu, and P. A. N. Machado, J. High Energy Phys. 07 (2015) 045.
[37] W. Shepherd, T. M. P. Tait, and G. Zaharijas, Phys. Rev. D **79**, 055022 (2009).
[38] M. E. Peskin and D. V. Schroeder, *An Introduction to Quantum Field Theory* (Westview Press, Boulder, CO, 1995).
[39] Y. Kats and M. D. Schwartz, J. High Energy Phys. 04 (2010) 016.
[40] D. Kahawala and Y. Kats, J. High Energy Phys. 09 (2011) 099.
[41] U. Ellwanger, C. Hugonie, and A. M. Teixeira, Phys. Rep. **496**, 1 (2010).
[42] B. C. Allanach *et al.*, Comput. Phys. Commun. **180**, 8 (2009).
[43] M. Farina, M. Perelstein, and B. Shakya, J. High Energy Phys. 04 (2014) 108.
[44] R. Franceschini and S. Gori, J. High Energy Phys. 05 (2011) 084.
[45] See [46] for a similar setup.
[46] X. Lu, H. Murayama, J. T. Ruderman, and K. Tobioka, Phys. Rev. Lett. **112**, 191803 (2014).
[47] CMS Collaboration, Report No. CMS-PAS-HIG-14-013, 2014.
[48] G. Aad *et al.* (ATLAS Collaboration), Eur. Phys. J. C **75**, 263 (2015).
[49] G. Aad *et al.* (ATLAS Collaboration), Eur. Phys. J. C **75**, 209 (2015); **75**, 370(E) (2015).
[50] Here we assume that the mass splitting between Higgisinos is small so that the neutralino and chargino can be treated as stable particles before they find each other and annihilate.
[51] M. Low and L.-T. Wang, J. High Energy Phys. 08 (2014) 161.
[52] O. D. Elbert, J. S. Bullock, S. Garrison-Kimmel, M. Rocha, J. Oñorbe, and A. H. G. Peter, Mon. Not. R. Astron. Soc. **453**, 29 (2015).
[53] A. H. G. Peter, M. Rocha, J. S. Bullock, and M. Kaplinghat, Mon. Not. R. Astron. Soc. **430**, 105 (2013).
[54] S. W. Randall, M. Markevitch, D. Clowe, A. H. Gonzalez, and M. Bradac, Astrophys. J. **679**, 1173 (2008).
[55] The derivatives in the operator do not cause any suppression of decay width, since the typical momentum of decay products is comparable to DM mass. One can also consider the scenario where the mediator is a vector boson, such as light dark photons. However, the decay in that case suffers additional suppressions from the dark photon mass due to the Landau-Yang theorem. Since the collider study is similar to the scalar channel, we do not consider it in this work.

[56] D. Curtin, Z. Surujon, and Y. Tsai, Phys. Lett. B **738**, 477 (2014).
[57] D. Curtin and Y. Tsai, J. High Energy Phys. 11 (2014) 136.
[58] Technical Report No. ATLAS-CONF-2015-044 (CERN, Geneva, 2015).
[59] G. Aad *et al.* (ATLAS Collaboration), Eur. Phys. J. C **75**, 92 (2015).
[60] G. Artoni, T. Lin, B. Penning, G. Sciolla, and A. Venturini, in *Community Summer Study 2013: Snowmass on the Mississippi (CSS2013), Minneapolis, 2013* (2013).
[61] G. Aad *et al.* (ATLAS Collaboration), Eur. Phys. J. C **75**, 299 (2015);**75**, 408(E) (2015).
[62] N. Zhou, D. Berge, L. Wang, D. Whiteson, and T. Tait, arXiv:1307.5327.
[63] D. Curtin, R. Essig, S. Gori, and J. Shelton, J. High Energy Phys. 02 (2015) 157.
[64] G. Aad *et al.* (ATLAS Collaboration), J. High Energy Phys. 11 (2014) 088.
[65] J. Alwall, M. Herquet, F. Maltoni, O. Mattelaer, and T. Stelzer, J. High Energy Phys. 06 (2011) 128.
[66] A. Alloul, N. D. Christensen, C. Degrande, C. Duhr, and B. Fuks, Comput. Phys. Commun. **185**, 2250 (2014).
[67] S. Chang, J. Galloway, M. Luty, E. Salvioni, and Y. Tsai, J. High Energy Phys. 03 (2015) 017.